JOURNAL OF SPACECRAFT AND ROCKETS
Vol. 46, No. 3, May–June 2009

Engineering Notes

ENGINEERING NOTES are short manuscripts describing new developments or important results of a preliminary nature. These Notes should not exceed 2500 words (where a figure or table counts as 200 words). Following informal review by the Editors, they may be published within a few months of the date of receipt. Style requirements are the same as for regular contributions (see inside back cover).

Stationkeeping of Geosynchronous Spacecraft Using a Hybrid Orbit Propagator and Optimization Technique

Tae Soo No*
Chonbuk National University, Chonju 560-756, Republic of Korea
and
Ok-Chul Jung† and Sang-Cherl Lee‡
Korea Aerospace Research Institute, Daejeon 305-333, Republic of Korea

DOI: 10.2514/1.40784

I. Introduction

WITH advances in space technology, current-generation geostationary spacecraft are often designed to operate for at least 10 years and are driven by multiple-mission scenarios. The ideal geostationary orbit has a constant semimajor axis, zero eccentricity, and zero inclination. These orbital elements, however, tend to deviate from the ideal values because of various perturbing forces, including the Earth's oblateness, the gravitational forces exerted by the sun and moon, the solar-wind pressure, etc. Therefore, stationkeeping (i.e., maintaining the position of a geostationary spacecraft within a designated longitude slot) becomes necessary, and the requirements for stationkeeping are becoming more stringent, not only because of the limited longitudinal resource, but also because of the real possibility of signal-frequency interference with neighboring spacecraft.

The objective of stationkeeping is to maintain the satellite within certain allowed limits for a given period of time. The classical strategy for stationkeeping is to separately control its position and velocity in two directions: that is, along the longitudinal and latitudinal directions (east–west and north–south stationkeeping, respectively). For example, drift-rate compensation targeting and the perigee sun-tracking method are used for east–west stationkeeping, whereas the inclination-vector drift is controlled for north–south stationkeeping [1,2]. Precise orbit propagation based on high-fidelity orbit models and accurate numerical integrators is used to plan an orbit-maneuver schedule in both directions within the constraints of the operator's work schedule.

This classical method is indirect in the sense that the values of the orbital elements are controlled based on predictions of the expected future trend of their variation rather than by directly controlling the spacecraft position. Therefore, the aim of this Note is to propose a method of directly controlling the position of a geostationary spacecraft for stationkeeping purposes. The advantages of highly precise numerical orbit propagation and the computational simplicity of an approximate closed-form analytical solution to the perturbed-geostationary-orbit problem are effectively combined to yield a so-called hybrid orbit propagator, which is used to predict spacecraft drift with respect to a reference position. We then proceed to plan stationkeeping such that a given cost function (e.g., fuel usage) is minimized while the spacecraft is maintained within the required stationkeeping limits. Highly nonlinear numerical simulation results are presented to illustrate the feasibility of the proposed method.

II. Hybrid Orbit Propagator

Orbit modeling using the relative motion between two neighboring orbits has been studied for orbit transfer and orbit rendezvous [3,4]. The motion in the real orbit is usually linearized with respect to a predefined reference orbit. Next, analytical solutions to the linearized equations of motion are obtained. For example, the Clohessy–Wiltshire (CW) equation has been used widely, but its application is limited because it does not include orbital perturbations [5–8].

In this Note, the orbit-compression method is used to describe the position of a geostationary spacecraft with respect to a reference longitude. Referring to Fig. 1, the component of the relative position vector $\delta \boldsymbol{r}$, defined as the difference between the real orbit $\boldsymbol{r}$ and the reference orbit $\boldsymbol{r}^*$, is expressed in terms of simple power-series and trigonometric functions. The kinds and number of functions used for this purpose have been adopted from [9], in which the approximate analytical solution to a perturbed-geostationary orbit is presented. Specifically, the following expression is used:

$$\begin{aligned}\delta x = {} & A_1 + A_2 t + A_3 t^2 + A_4 \sin \omega_e t + A_5 \sin 2\omega_e t + A_6 \sin 3\omega_e t \\ & + A_7 \cos \omega_e t + A_8 \cos 2\omega_e t + A_9 \cos 3\omega_e t + A_{10} \sin \Omega_s t \\ & + A_{11} \sin 2\Omega_s t + A_{12} \sin 3\Omega_s t + A_{13} \cos \Omega_s t + A_{14} \cos 2\Omega_s t \\ & + A_{15} \cos 3\Omega_s t + A_{16} \sin \Omega_m t + A_{17} \sin 2\Omega_m t \\ & + A_{18} \sin 3\Omega_m t + A_{19} \cos \Omega_m t + A_{20} \cos 2\Omega_m t \\ & + A_{21} \cos 3\Omega_m t + A_{22} t \sin \omega_e t + A_{23} t \cos \omega_e t + A_{24} \sin \omega_m t \\ & + A_{25} \sin 2\omega_m t + A_{26} \cos \omega_m t + A_{27} \cos 2\omega_m t \end{aligned} \tag{1}$$

where δx is the component of $\delta \boldsymbol{r}$ in the radial direction in the CW frame [10]. The same expressions are used for the other two components, δy and δz, respectively, in the along-track and cross-track directions. In Eq. (1), ω_e is the angular speed of the Earth's rotation, ω_s is the sun's orbital rate, ω_m is the moon's orbital rate, $\Omega_s = \omega_s - \omega_e$, and $\Omega_m = \omega_m - \omega_e$.

The 27 coefficients in Eq. (1) are determined using a least-squares regression method to find the best fit to the residual vector $\delta \boldsymbol{r}$. To this aim, the equations of the orbital motion of a geostationary spacecraft

Presented as Paper 5331 at the 24th AIAA International Communications Satellite Systems Conference, San Diego, CA, 11–14 June 2006; received 4 September 2008; revision received 24 February 2009; accepted for publication 24 February 2009.

*Professor, Department of Aerospace Engineering, 664-14 Deokjin-dong, Deokjin-gu, Chonju.
†Researcher, Satellite Mission Operations Department, 45 Eoeun-Dong, Yuseong-gu, Daejeon.
‡Senior Researcher, Communication, Ocean and Meteorology Satellite Program Office, 45 Eoeun-Dong, Yuseong-gu, Daejeon.

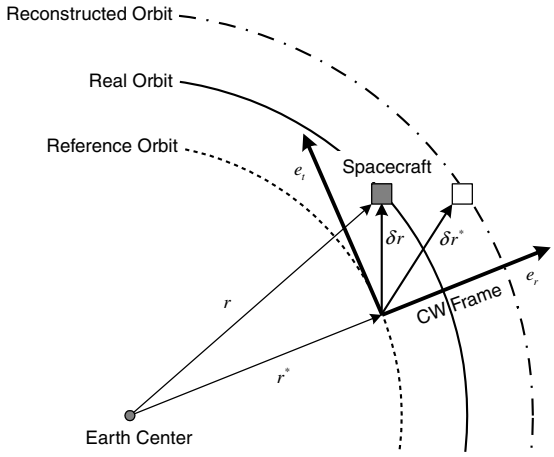

Fig. 1 Definition of the real and reference orbits.

are integrated to generate its positional drift $\boldsymbol{r}$ over a specified time period. Perturbations due to the various sources are included as needed, and an advanced numerical scheme may be applied to obtain the precise orbit-propagation results. Choosing the ideal geostationary orbit as the reference orbit, we then obtain the real position residual vector, as

$$\delta \boldsymbol{r} = \boldsymbol{r} - \boldsymbol{r}^* \tag{2}$$

where $\boldsymbol{r}^*$ is the position vector of the reference orbit, which is a constant vector in the CW frame. Next, the components of the real residual vector $\delta \boldsymbol{r}$ are transformed into the CW frame and its results are used to find the 27 coefficients in Eq. (1). The position residual vector thus obtained is called the reconstructed residual vector $\delta \boldsymbol{r}^*$.

Once the reconstructed residual vector is available, its computation is trivial, because its components are all expressed explicitly in terms of time and algebraic and trigonometric functions. Here, the only concern is its accuracy compared with the precisely generated real orbit. Figure 2 shows the difference in position components as a function of time, generated using precise orbit propagation and the hybrid orbit propagator. Perturbing forces due to the Earth's gravity up to J_4, the sun/moon attraction, and the solar-wind pressure are all included. It is evident that the error remains below 0.5 km for 14 days, which would be sufficient for the purposes of stationkeeping planning.

III. Stationkeeping Planning

The main purpose of stationkeeping is to maintain the spacecraft within a predefined longitude and/or latitude limit. Therefore, orbit-correction maneuvers must be regularly performed to compensate for natural perturbations that act to change the orbit. As discussed in the previous section, the classical strategy is to maintain the values of the orbital elements within the specified limits for a given period. However, as discussed in this Note, one can directly control the position components with respect to the reference longitude, because their natural drift due to the perturbing forces as a function of time are readily determined from Eq. (1). If we assume that the orbit is impulsively corrected and that the effect can be added linearly to the reconstructed residual vector $\delta \boldsymbol{r}^*$, then the total drift $\delta \mathbf{r}(t)$ can be expressed as

$$\delta \mathbf{r}(t) = \delta r^*(t) + \sum_{i=1}^{N} \boldsymbol{\Phi}(t - T_i) \Delta \boldsymbol{V}_i u(t - T_i) \tag{3}$$

where N denotes the number of impulsive burns, T_i is the time at impulsive burn, $\boldsymbol{\Phi}(\tau)$ is the state-transition matrix that maps the effect of impulsive velocity increments into the future, and $u(\tau)$ is a unit step function, which is 1 if τ is greater than zero, and 0 otherwise. For the state-transition matrix $\boldsymbol{\Phi}(\tau)$, we have adopted the classical expression [11]:

$$\boldsymbol{\Phi}(\tau) = \frac{1}{\omega_e} \begin{bmatrix} \sin \omega_e \tau & 2(1 - \cos \omega_e \tau) & 0 \\ 2(\cos \omega_e \tau - 1) & 4 \sin \omega_e \tau - 3\omega_e \tau & 0 \\ 0 & 0 & \sin \omega_e \tau \end{bmatrix} \tag{4}$$

Stationkeeping planning now becomes a simple problem of choosing the number of burns N, the direction and magnitude of $\Delta \boldsymbol{V}_i$, and the time at burn T_i. Note that stationkeeping in the east–west direction can be decoupled from that along the north–south direction. However, any stationkeeping plan must ensure that the spacecraft remains within the predefined tolerance box during the entire stationkeeping period T_{SK}. Mathematically, the following constraints should be satisfied:

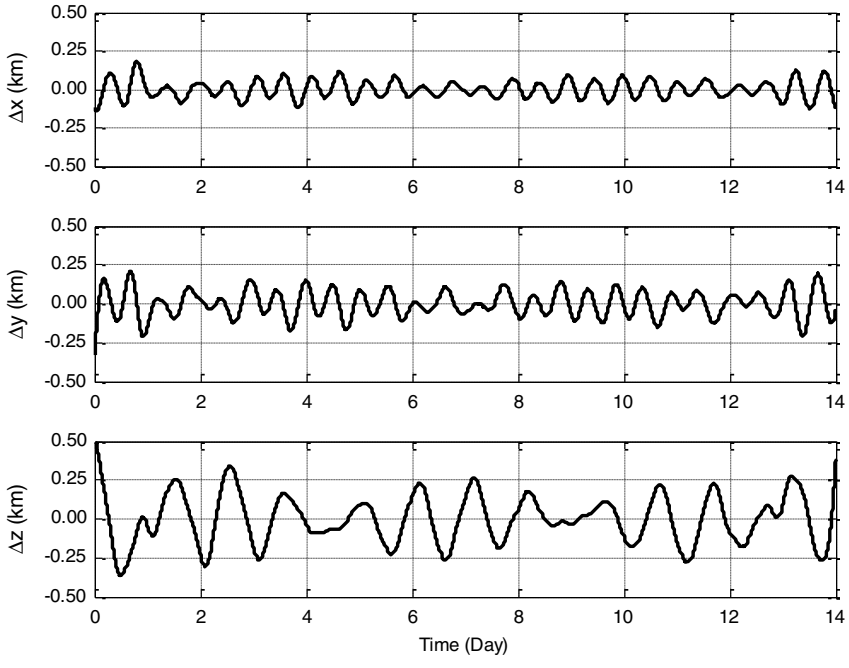

Fig. 2 Orbit-propagation error.

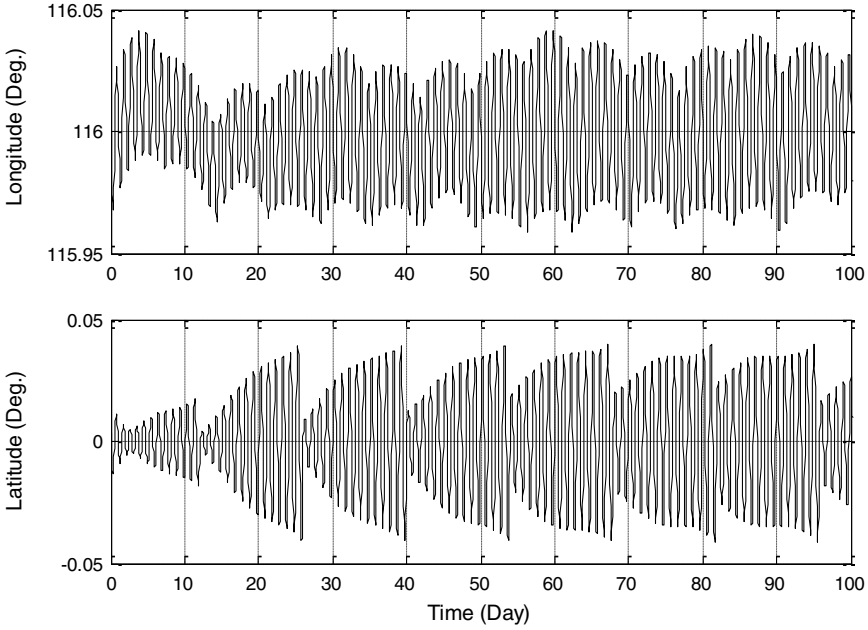

Fig. 3 Spacecraft longitude and latitude as a function of time: minimum-fuel stationkeeping.

$$
\begin{aligned}
&|\delta\mathbf{x}(t)| < \delta x_{\max} \qquad t_0 < t < t_0 + T_{\mathrm{SK}} \\
&|\delta\mathbf{y}(t)| < \delta y_{\max} \qquad t_0 < t < t_0 + T_{\mathrm{SK}} \\
&|\delta\mathbf{z}(t)| < \delta z_{\max} \qquad t_0 < t < t_0 + T_{\mathrm{SK}}
\end{aligned} \tag{5}
$$

where t_0 is the start time of the stationkeeping cycle; $\delta\mathbf{x}(t)$, $\delta\mathbf{y}(t)$, and $\delta\mathbf{z}(t)$ are components of the total drift $\delta\mathbf{r}(t)$, as defined in Eq. (3); and $\delta x_{\max}$, $\delta y_{\max}$, and $\delta z_{\max}$ denote the maximum-allowable position drift along the radial, longitudinal, and cross-track directions in the CW frame.

Many solutions exist that satisfy the objectives of the stationkeeping strategy discussed previously. Noting that the mission lifetime of a geostationary spacecraft depends directly on the fuel consumed for stationkeeping, one useful choice from many alternatives is that which minimizes the following objective function:

$$J = \sum_{i=1}^{N} |\Delta \boldsymbol{V}_i|^2 \tag{6}$$

Stationkeeping planning then becomes a simple constrained optimization problem. In other words, one should find a set of $(T_i, \Delta \boldsymbol{V}_i)$ that satisfies Eq. (5) while minimizing Eq. (6). This method is referred to here as *minimum-fuel stationkeeping*.

As the number of geostationary spacecraft increases, one must operate several spacecraft simultaneously within a designated longitude slot. This increases the chance of collision, meaning that spacecraft positions must be tightly controlled. For this purpose, one may use the solution that minimizes the maximum deviation from the reference longitude, as

$$\text{Minimize the max of} \quad |\delta\mathbf{r}(\mathrm{t})| \qquad t_0 < t < t_0 + T_{\mathrm{SK}} \tag{7}$$

We call this method *minimum-distance stationkeeping*.

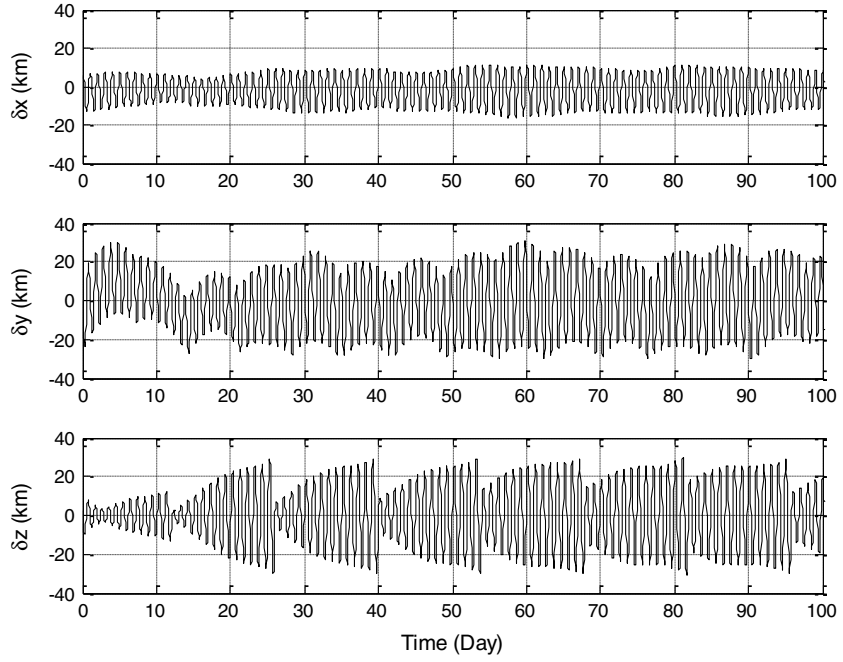

Fig. 4 Spacecraft position component in the CW frame as a function of time: minimum-fuel stationkeeping.

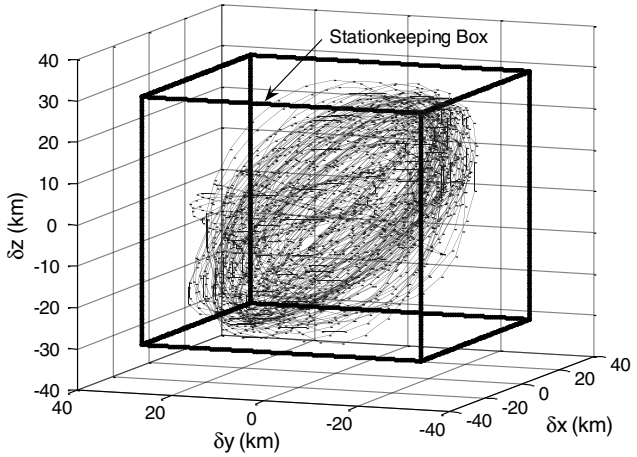

Fig. 5 Three-dimensional spacecraft trajectory: minimum-fuel stationkeeping.

IV. Nonlinear Simulation Examples and Discussion

A. Minimum-Fuel Stationkeeping

Nonlinear simulations have been performed to illustrate the use of the stationkeeping method proposed here. Stationkeeping in the east–west and north–south directions is planned separately, because the motion along the respective directions is uncoupled in the linear sense. A two-burn once-a-week maneuver is used for east–west stationkeeping, whereas a biweekly one-burn maneuver is used for north–south stationkeeping [12,13]. The directions of the impulsive burns for east–west and north–south maneuvers are, respectively, confined to the along-track and cross-track directions.

Considering these operational restrictions, the cost function to be minimized for east–west stationkeeping planning is

$$J_{\mathrm{EW}} = |\Delta V_{1,\mathrm{EW}}|^2 + |\Delta V_{2,\mathrm{EW}}|^2 \tag{8}$$

To constrain the conditions required for east–west stationkeeping, we use only the y component in Eq. (5), because the purpose of east–west stationkeeping is to control the position drift in the longitudinal direction, and the x component can be controlled indirectly through the coupling effect. Therefore, after substituting Eq. (4) into Eq. (3), we can write the constraint equations as

$$\left|\delta y^*(t) + \sum_{i=1}^{2}[4\sin\omega_e(t - T_{i,\mathrm{EW}}) - 3\omega_e(t - T_{i,\mathrm{EW}})]\Delta V_{i,\mathrm{EW}}u(t - T_{i,\mathrm{EW}})\right| < \delta y_{\max} \qquad t_0 < t < t_0 + 1 \text{ week} \tag{9}$$

where $\delta y^*(t)$ is the along-track component of the reconstructed residual vector $\delta\boldsymbol{r}^*$, and $T_{i,\mathrm{EW}}$ and $\Delta V_{i,\mathrm{EW}}$ are, respectively, the time at orbit maneuver and the required velocity increment for east–west stationkeeping. For the north–south direction, the equivalent cost function and constraint equations are, respectively,

$$J_{\mathrm{NS}} = |\Delta V_{1,\mathrm{NS}}|^2 \tag{10}$$

and

$$|\delta z^*(t) + \sin\omega_e(t - T_{1,\mathrm{NS}})\Delta V_{1,\mathrm{NS}}u(t - T_{1,\mathrm{NS}})| < \delta z_{\max} \qquad t_0 < t < t_0 + 2 \text{ week} \tag{11}$$

where $\delta z^*(t)$ is the cross-track component of the reconstructed residual vector $\delta\boldsymbol{r}^*$, and $T_{1,\mathrm{NS}}$ and $\Delta V_{1,\mathrm{NS}}$ are, respectively, the time at orbit maneuver and the required velocity increment for north–south stationkeeping.

Figures 3–5 show the nonlinear simulation results of minimum-fuel east–west and north–south stationkeeping for 100 days. A simulation code based on MATLAB® was written for this purpose. As for the optimization solver, we used `fmincon` and `fminmax` functions, available from MATLAB's Optimization Toolbox. Perturbing forces due to the Earth's gravity up to J_4, the sun/moon attraction, and the solar-wind pressure are all included, as these are the primary sources that cause spacecraft drift in the longitudinal and lateral directions.

For example purposes, the nominal longitude is set to 116°E, and the spacecraft's position is to be controlled within ±0.05° in both longitude and latitude. This tolerance angle corresponds to approximately 37 km in both the longitudinal and cross-track positions in the stationkeeping box. However, for simplicity, we set $y_{\max} = z_{\max} = 30$ km in the simulation. From Fig. 3, it is clear that the spacecraft longitude and latitude do not exceed the allowed limits. Figures 4 and 5 show the spacecraft trajectory in the stationkeeping box. The spacecraft does not drift beyond 30 km in any direction. Note that the radial x position is also sufficiently under control. The required velocity changes in the east–west and north–south directions, which are the result of stationkeeping planning, are summarized in Table 1.

Table 1 Stationkeeping plan result

	Case 1: minimum-fuel strategy (9.6041 m/s total)			Case 2: minimum-distance strategy (11.3852 m/s total)		
	East—west		North—south	East—west		North—south
Week	$\lvert\Delta V_{1,\mathrm{EW}}\rvert$, m/s	$\lvert\Delta V_{2,\mathrm{EW}}\rvert$, m/s	$\lvert\Delta V_{\mathrm{NS}}\rvert$, m/s	$\lvert\Delta V_{1,\mathrm{EW}}\rvert$, m/s	$\lvert\Delta V_{2,\mathrm{EW}}\rvert$, m/s	$\lvert\Delta V_{\mathrm{NS}}\rvert$, m/s
1	0.0119	0.0111	——	0.0640	0.0244	——
2	0.0268	0.0251	0.8469	0.0362	0.0047	2.0206
3	0.0224	0.0210	——	0.0462	0.0009	——
4	0.0167	0.0157	1.8012	0.0034	0.0305	1.9357
5	0.0425	0.0041	——	0.0548	0.0172	——
6	0.0420	0.0003	1.5996	0.0352	0.0066	1.6880
7	0.0375	0.0060	——	0.0495	0.0050	——
8	0.0185	0.0157	1.2189	0.0170	0.0168	1.4285
9	0.0533	0.0160	——	0.0622	0.0237	——
10	0.0211	0.0201	1.1610	0.0356	0.0064	1.1842
11	0.0638	0.0201	——	0.0564	0.0131	——
12	0.0171	0.0162	0.9982	0.0226	0.0110	1.1611
13	0.0461	0.0051	——	0.0679	0.0303	——
14	0.0179	0.0166	1.3477	0.0393	0.0040	1.1821
Subtotal	0.4376	0.1931	8.9735	0.5904	0.1945	10.6003

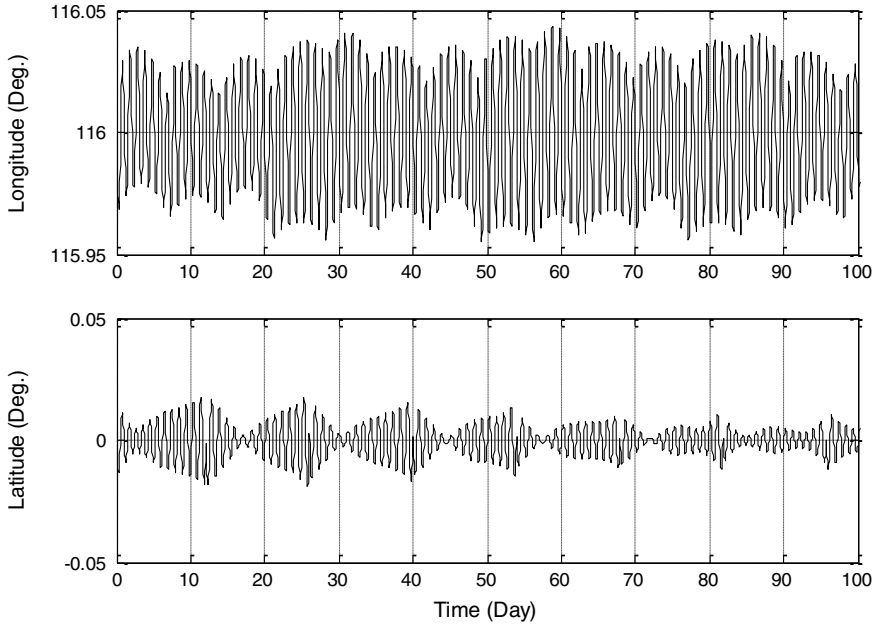

Fig. 6 Spacecraft longitude and latitude as a function of time: minimum-distance stationkeeping.

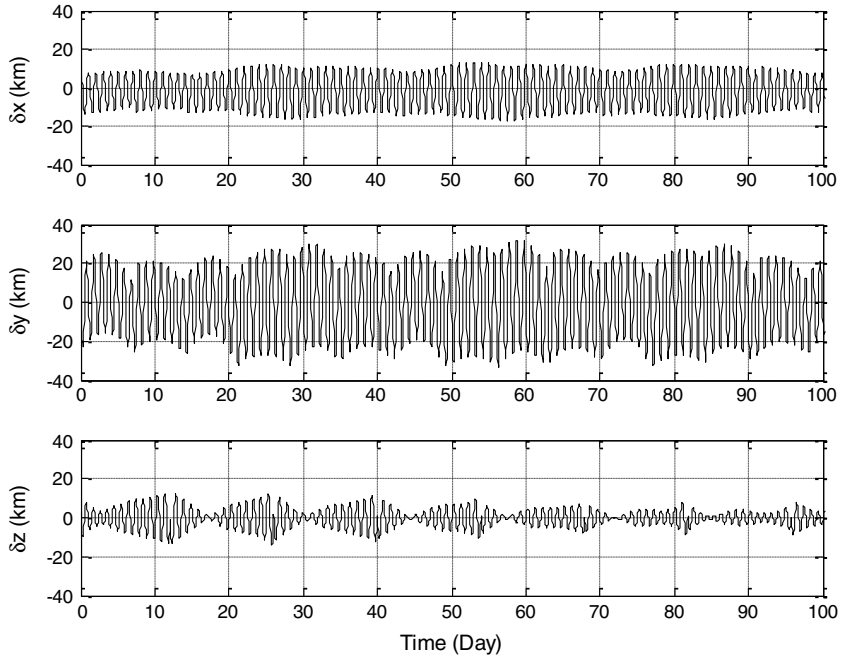

Fig. 7 Spacecraft position in the CW frame as a function of time: minimum-distance stationkeeping.

B. Minimum-Distance Stationkeeping

The only changes required for minimum-distance stationkeeping planning are the cost functions to be minimized: for example, for east–west stationkeeping,

$$J_{\mathrm{EW}} = \max \text{ of } \left| \delta y^*(t) + \sum_{i=1}^{2} [4 \sin \omega_e (t - T_{i,\mathrm{EW}}) - 3\omega_e (t - T_{i,\mathrm{EW}})] \Delta V_{i,\mathrm{EW}} u(t - T_{i,\mathrm{EW}}) \right|^2 \tag{12}$$

and for north–south stationkeeping,

$$J_{\mathrm{NS}} = \max \text{ of } |\delta z^*(t) + \sin \omega_e (t - T_{1,\mathrm{NS}}) \Delta V_{1,\mathrm{NS}} u(t - T_{1,\mathrm{NS}})|^2 \tag{13}$$

Equations (9) and (11) are still applied as a set of constraint conditions.

The simulation results are shown in Figs. 6–8. As for minimum-fuel stationkeeping, the spacecraft longitude and latitude and, equivalently, its position in the stationkeeping box are well controlled. We can clearly see that the spacecraft position along the cross-track direction is more tightly controlled compared with the minimum-fuel stationkeeping case. However, 100 days of stationkeeping using the minimum-distance stationkeeping method requires 18% more fuel than that required when adopting the minimum-fuel stationkeeping strategy.

V. Conclusions

This Note proposed a new method for geostationary-spacecraft stationkeeping planning. A hybrid orbit propagator, a combination of

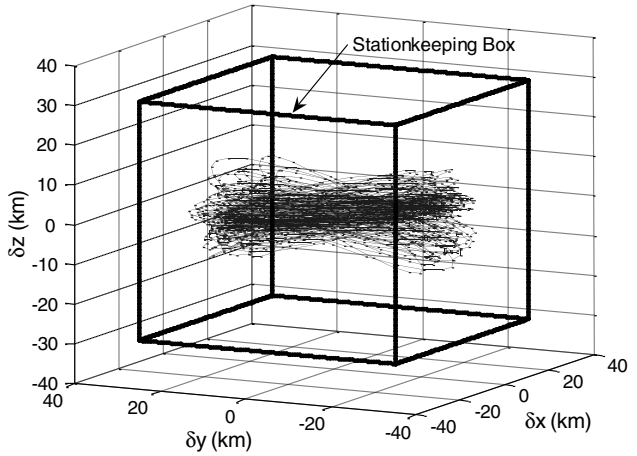

Fig. 8 Three-dimensional spacecraft trajectory: minimum-distance stationkeeping.

a precise numerical orbit propagator and an approximate analytical orbit propagator, is used to predict spacecraft position drift arising from various perturbing forces. Stationkeeping planning is formulated in the framework of an optimization problem. To save fuel and to reduce the chance of collision with nearby spacecraft, we presented two methods for stationkeeping planning: minimum-fuel and minimum-distance stationkeeping. We applied these methods to a typical geostationary spacecraft and performed nonlinear simulations. The simulation results clearly show that both methods can be used to control the spacecraft position within the 3-D stationkeeping box limits.

Acknowledgment

This work was supported by the STSAT-3 Program grant of the Ministry of Education, Science, and Technology.

References

[1] Soop, E. M., *Handbook of Geostationary Orbits*, 3rd ed., Kluwer Academic, Norwell, MA, 1994, Chaps. 6–7.

[2] Pocha, J. J., *An Introduction to Mission Design for Geostationary Satellites*, Space Technology Library, D. Reidel, Boston, 1983.

[3] Melton, R., "Time-Explicit Representation of Relative Motion Between Elliptical Orbits," *Journal of Guidance, Control, and Dynamics*, Vol. 23, No. 4, 2000, pp. 604–610. doi:10.2514/2.4605

[4] Chichka, D. F., "Satellite Clusters with Constant Apparent Distribution," *Journal of Guidance, Control, and Dynamics*, Vol. 24, No. 1, 2001, pp. 117–122. doi:10.2514/2.4683

[5] Carter, T. E., "State Transition Matrix for Terminal Rendezvous Studies: Brief Survey and New Example," *Journal of Guidance, Control, and Dynamics*, Vol. 21, No. 1, 1998, pp. 148–155. doi:10.2514/2.4211

[6] Hoots, F. R., and France, R. G., "Hybrid Ephemeris Compression Model," Astrodynamics Specialist Conference, AAS/AIAA Paper 97-689, 1997.

[7] Hoots, F. R., and Segerman, A. M., "Satellite Ephemeris Representation Using Hybrid Compression," *Proceedings of the AAS/AIAA Space Flight Mechanics Meeting*, American Astronautical Society, Springfield, VA, 2002, pp. 429–439.

[8] Deok-Jin Lee, Tae Soo No, Seok-Woo Choi, Sang-Ryul Lee, Hak-Jung Kim, and Kyle T. Alfriend, "Precise Ephemeris Reconstruction Method Using CW Frame and Multiple Sequential Compression," *Journal of Guidance, Control, and Dynamics*, Vol. 26, No. 5, 2003, pp. 781–785. doi:10.2514/2.5112

[9] No, T. S., and Jung, O. C., "Analytical Solution to Perturbed Geosynchronous Orbit," *Acta Astronautica*, Vol. 56, No. 7, 2005, pp. 641–651. doi:10.1016/j.actaastro.2004.11.008

[10] Clohessy, W. H., and Wiltshire, R. S., "Terminal Guidance System for Satellite Rendezvous," *Journal of the Aerospace Sciences*, Vol. 27, No. 9, 1960, pp. 653–658.

[11] Prussing, J. E., and Conway, B. A., *Orbital Mechanics*, Oxford Univ. Press, Oxford, 1993.

[12] Chobotov, V. A., *Orbital Mechanics*, 2nd ed., AIAA, Reston, VA, 1996.

[13] No, T. S., "Simple Approach to East-West Station Keeping of Geosynchronous Spacecraft," *Journal of Guidance, Control, and Dynamics*, Vol. 22, No. 5, 1999, pp. 734–736. doi:10.2514/2.4447

D. Spencer
Associate Editor